

# MODELING STYRENE HYDROGENATION KINETICS USING PALLADIUM CATALYSTS

G. T. Justino<sup>1</sup>, C. S. A. Vale<sup>1</sup>, M. A. P. da Silva<sup>1\*</sup> and A. R. Secchi<sup>2</sup>

<sup>1</sup>Escola de Química, UFRJ, Av. Athos da Silveira Ramos, 149 Bloco E,  
Ilha do Fundão, CEP: 21941-909, Rio de Janeiro - RJ, Brazil.  
Phone: (55) (21) 3938-7606; Fax: (55) (21) 3938-7567  
E-mail: monica@eq.ufrj.br

<sup>2</sup>Programa de Engenharia Química, COPPE, Universidade Federal do  
Rio de Janeiro, Rio de Janeiro - RJ, Brazil

(Submitted: February 25, 2015 ; Revised: August 28, 2015 ; Accepted: October 9, 2015)

**Abstract** - The high octane number of pyrolysis gasoline (PYGAS) explains its insertion in the gasoline pool. However, its use is troublesome due to the presence of gum-forming chemicals which, in turn, can be removed via hydrogenation. The use of Langmuir-Hinshelwood kinetic models was evaluated for hydrogenation of styrene, a typical gum monomer, using Pd/9%Nb<sub>2</sub>O<sub>5</sub>-Al<sub>2</sub>O<sub>3</sub> as catalyst. Kinetic models accounting for hydrogen dissociative and non-dissociative adsorption were considered. The availability of one or two kinds of catalytic sites was analyzed. Experiments were carried out in a semi-batch reactor at constant temperature and pressure in the absence of transport limitations. The conditions used in each experiment varied between 16 – 56 bar and 60 – 100 °C for pressure and temperature, respectively. The kinetic models were evaluated using MATLAB and EMSO software. Models using adsorption of hydrogen and organic molecules on the same type of site fitted the data best.

**Keywords:** Pyrolysis gasoline; Hydrotreatment; Styrene; Kinetic models.

## INTRODUCTION

Pyrolysis gasoline (PYGAS) is a side product of petroleum naphtha pyrolysis. It is a mixture of C<sub>5</sub> to C<sub>12</sub> hydrocarbons, the main components being BTX aromatics (benzene, toluene, and xylene). Styrene, mono and diolefins are also present in PYGAS in appreciable proportions. The high octane number of PYGAS is responsible for its insertion in the gasoline pool (Nijhuis *et al.*, 2003).

However, the gum-forming properties of styrene, mono and diolefins hinders its actual participation on the gasoline pool. Compounds containing sulfur and nitrogen also need to be removed from PYGAS (Ali, 2012). In addition to that, recent changes in envi-

ronmental legislation in Brazil now require much lower concentrations of aromatics in gasoline, thus demanding development of processes for this end (Gaspar *et al.*, 2008).

The best way to get rid of these chemicals while maintaining the high octane number of PYGAS is via a selective hydrogenation process, which occurs in two stages (Cheng *et al.*, 1986; Rojas and Zeppieri, 2014). In the first one, styrene and diolefins are selectively hydrogenated under moderate conditions to prevent gum and coke formation. The reactor temperature and hydrogen pressure are in the range of 50 – 130 °C and 20 – 40 bar, respectively (Cheng *et al.*, 1986; Medeiros *et al.*, 2007). In the second stage, sulfur compounds are converted and mono-olefins are

\*To whom correspondence should be addressed

This is an extended version of the work presented at the 20th Brazilian Congress of Chemical Engineering, COBEQ-2014, Florianópolis, Brazil.

hydrogenated using higher temperatures (Mostoufi *et al.*, 2005). Currently, the first stage is carried out using Pd catalysts while the second uses CoMo/Al<sub>2</sub>O<sub>3</sub> regenerable catalysts (Cheng *et al.*, 1986; Gaspar *et al.*, 2008). It is well established that, during the first stage, hydrogenation of mono-olefins is not significant, since selectivity to adsorption onto Pd catalytic sites is much greater for diolefins as compared to mono-olefins. Thus, hydrogenation of mono-olefins occurs only after reducing of diolefins concentration.

The first hydrogenation stage is sufficient for the production of a stable mixture with high octane number, which can be added to the gasoline pool. Further processing in the second stage normally occurs when PYGAS is used for aromatic extraction. If the objective is the insertion in the gasoline pool, this stage can be by-passed, unless the initial composition of the PYGAS and the local legislation require a further reducing in aromatics and sulfur concentration (Cheng *et al.*, 1986; Ali, 2012).

In this work, PYGAS was simulated with a solution of styrene in toluene. Styrene was selected as a model molecule regarding PYGAS since it is one of the less reactive of its components (Cheng *et al.*, 1986; Nijhuis *et al.*, 2003; Gaspar *et al.*, 2008).

The kinetic parameters of PYGAS hydrogenation over a Pd/Al<sub>2</sub>O<sub>3</sub> catalyst were initially investigated by Cheng *et al.* (1986) using a power-law model which assumed an order of reaction equal to 1 for both styrene and hydrogen. Ali (2012) also assumed first order with respect to styrene and estimated as 0.1 the order of reaction for hydrogen, and Tukac *et al.* (2007) estimated order 1 for hydrogen and 0.5 for styrene. Jackson and Shaw (1996) found a completely different result for styrene hydrogenation over a Pd/carbon catalyst: assuming zero order for hydrogen, they estimated also zero order for styrene. This result might indicate that Langmuir-Hinshelwood models could be a good representation for the reaction rate.

Kinetic studies of PYGAS hydrogenation over Pd/Al<sub>2</sub>O<sub>3</sub> and Pd-Ni/Al<sub>2</sub>O<sub>3</sub> catalyst were investigated by Zhou *et al.* (2007; 2010) and Abreu *et al.* (2013), respectively. Mixtures of styrene, olefins and diolefins were employed to represent PYGAS. These authors obtained good fits for styrene hydrogenation using Langmuir-Hinshelwood models considering dissociative hydrogen adsorption and the existence of two kinds of catalytic sites for the adsorption of organic compounds and hydrogen. Styrene hydrogenation was also carried out in a trickle-bed reactor over Pd/Al<sub>2</sub>O<sub>3</sub> by Nijhuis *et al.* (2003) and Fraga (2009). These authors obtained good fits with Lang-

muir-Hinshelwood models considering the non-dissociative mechanism for hydrogen adsorption.

Recently, the effects of supports for Pd catalyst have been studied for PYGAS hydrogenation. Gaspar *et al.* (2008) investigated the addition of ZrO<sub>2</sub> in different loadings on Al<sub>2</sub>O<sub>3</sub> for hydrogenation of a model mixture representative of PYGAS. However, the Pd/Al<sub>2</sub>O<sub>3</sub> catalyst was still the most active. Zeng *et al.* (2009) tested a Pd catalyst on macro-mesoporous TiO<sub>2</sub> and obtained satisfactory results when compared with a Pd/TiO<sub>2</sub> catalyst of microporous morphology. Corvaisier *et al.* (2013) evaluated different metal catalysts supported on SiO<sub>2</sub> for styrene hydrogenation, obtaining highest activity for Pd/SiO<sub>2</sub>, but no comparison with the traditional Pd/Al<sub>2</sub>O<sub>3</sub> catalyst was made. These authors obtained a good fit with a Langmuir-Hinshelwood model considering the dissociative adsorption of hydrogen and only one type of catalytic site was tested.

Betti *et al.* (2016) investigated styrene hydrogenation using a palladium catalyst supported on an inorganic-organic composite. Horiuti-Polanyi and Langmuir-Hinshelwood mechanisms were considered for hydrogenation and adsorption, respectively. The best fit was obtained for the model considering the competitive adsorption of all compounds, only one type of catalytic site, and dissociative adsorption of hydrogen.

Previous work of the group (Vale, 2013) studied the niobia-modified alumina-supported palladium catalyst (x Nb<sub>2</sub>O<sub>5</sub>-Al<sub>2</sub>O<sub>3</sub>, with 9% and 18% of Nb<sub>2</sub>O<sub>5</sub> in weight) and the effects on styrene hydrogenation when compared to Pd/Al<sub>2</sub>O<sub>3</sub>. The most active catalyst was the one with 9% w/w of niobia. Consequently, in the present work the Pd/9%Nb<sub>2</sub>O<sub>5</sub>-Al<sub>2</sub>O<sub>3</sub> catalyst was chosen to evaluate the kinetic models for styrene hydrogenation. Kinetic parameters of the power-law and Langmuir-Hinshelwood models were estimated based on experiments carried out in a semi-batch bench scale reactor.

## EXPERIMENTAL

### Catalyst

The composition of the catalyst was 1% w/w of palladium and 9% w/w of Nb<sub>2</sub>O<sub>5</sub>. Palladium dispersion was determined as 13% by hydrogen chemisorption assuming a 1:2 (H<sub>2</sub>:Pd) ratio. Specific area and pore volume, obtained using nitrogen adsorption, were 179 m<sup>2</sup>/g and 0.47 cm<sup>3</sup>/g, respectively (Alegre *et al.*, 2006).

## Styrene Solution Preparation

Initially, styrene was purified to eliminate tert-butyl-catechol, a stabilizer which is known to interfere with the catalyst activity (Hoffer *et al.*, 2004; Wen *et al.*, 2013). Toluene, used as solvent, was also purified for the removal of water since it decreases the reaction rate (Wolffenbuttel *et al.*, 2001). Solutions of styrene in toluene were prepared right before each catalytic test, with concentrations ranging from 0.3 to 0.8 mol/L.

## Styrene Hydrogenation

Styrene hydrogenation was carried out in a Parr reactor (0.160 L) operated at 600 rpm under constant temperature and pressure. The Pd/9%Nb<sub>2</sub>O<sub>5</sub>-Al<sub>2</sub>O<sub>3</sub> catalyst was prepared by impregnation. The detailed experimental procedure is presented elsewhere (Alegre *et al.*, 2006). The catalyst Pd/9%Nb<sub>2</sub>O<sub>5</sub>-Al<sub>2</sub>O<sub>3</sub> (approximately 0.0150 g) was previously reduced *in situ* under pure H<sub>2</sub> (10 bar) at 150 °C for 1 hour. After reduction, the reactor was cooled to room temperature. Then, 0.105 L of reaction mixture was introduced into the reactor under H<sub>2</sub> atmosphere, which was then heated to the desired temperature. Next, the zero<sup>th</sup> aliquot was taken, the reactor was pressurized and the agitation (600 rpm) initiated. The experimental conditions were chosen to reduce the effects of mass transport limitations. Aliquots taken at intervals of 5 min during 1 h of reaction were analyzed in a HP 6890N chromatograph, equipped with a DB1 column (60 m X 0.32 mm) and a flame ionization detector (FID).

Two sets of experiments were carried out to estimate kinetic parameters of the studied models. In the first set of experiments, the temperature was fixed at 80 °C, which is inside the temperature range of 50 – 130 °C used industrially (Medeiros *et al.*, 2007). Five levels of H<sub>2</sub> pressure (16, 26, 36, 46, and 56 bar) and three levels of styrene concentration (0.3, 0.5 and 0.8 mol/L) were used. The parameter estimation using this first data set resulted in the knowledge of the expected values for the equilibrium constants of adsorption at the reference temperature ( $T_R$ ) and for the pre-screening of the kinetic models.

The second set of experiments includes the effects of temperature on the styrene hydrogenation with five levels (60, 70, 80, 90, and 100 °C). In this set, the effects of H<sub>2</sub> pressure were evaluated at the same five levels mentioned previously, and the initial styrene concentration was kept at 0.5 mol/L in all these new experiments. With this additional set of experiments, it was also possible to estimate the

apparent activation energy and heats of adsorption of styrene, hydrogen and ethylbenzene.

## KINETIC MODELING

All measurements were carried out in the kinetic regime. The external diffusion effect was eliminated by a sufficiently effective stirring, and the pore diffusion effect was eliminated by the use of a sufficiently small particle size.

The molar balances can be written as follows:

$$(-r_s) = -\frac{V}{m_{cat}} \frac{dC_s}{dt} \quad (1)$$

$$r_e = \frac{V}{m_{cat}} \frac{dC_e}{dt} \quad (2)$$

where:

$(-r_s)$  = rate of disappearance of styrene (mol/(min g<sub>cat</sub>));

$r_e$  = rate of formation of ethylbenzene (mol/(min g<sub>cat</sub>));

$C_s$  and  $C_e$  = styrene and ethylbenzene concentrations (mol/L);

$m_{cat}$  = catalyst mass (g<sub>cat</sub>);

$V$  = volume of reaction mixture (L).

Two power-law models were fitted to the styrene hydrogenation data, using the rate expressions shown in Table 1. Model PL<sub>αβ</sub> gives individual reaction orders for styrene and hydrogen. Model PL<sub>β</sub> imposes first-order kinetics regarding styrene, allowing the H<sub>2</sub> order to be determined.

**Table 1: Power-law kinetic models.**

Model	Rate equation ( $-r_s$ )
PL <sub>αβ</sub>	$kC_s^\alpha C_H^\beta$
PL <sub>β</sub>	$kC_s C_H^\beta$

Langmuir-Hinshelwood models with three and four parameters were also evaluated, considering the surface reaction of adsorbed species as the limiting step. The evaluated models consider adsorption of organic compounds and hydrogen on the same type of active site or on two types of active sites (one of which adsorbs hydrogen and the other adsorbs organic molecules). The corresponding rate expressions are shown in Tables 2 and 3, where  $k$  is the specific rate and  $K_i$  and  $C_i$  are, respectively, the

adsorption constant and the concentration of compounds  $i$  (styrene, ethylbenzene, or hydrogen). In the nomenclature of the kinetic models, the Roman numerals represent the number of types of active sites, and the prefixes account for the dissociative mechanism of hydrogen adsorption (models D), as well as for the non-dissociative one (models ND). The suffixes S, E and H represent the inclusion in the rate expression of the corresponding adsorption terms for styrene, ethylbenzene and hydrogen, respectively, in the denominator.

**Table 2: Langmuir-Hinshelwood kinetic models with three parameters.**

Model	Rate equation ( $-r_s$ )	$K_{global}$
ND_I_SE	$\frac{K_{global}C_H C_s}{(1 + K_s C_s + K_e C_e)^2}$	$kK_s K_H$
D_I_SE	$\frac{K_{global}C_H C_s}{(1 + K_s C_s + K_e C_e)^3}$	$kK_s K_H$
ND_II_SE	$\frac{K_{global}C_H C_s}{(1 + K_s C_s + K_e C_e)}$	$kK_s K_H$
D_II_SE	$\frac{K_{global}\sqrt{C_H C_s}}{(1 + K_s C_s + K_e C_e)}$	$kK_s \sqrt{K_H}$
ND_I_SH	$\frac{K_{global}C_H C_s}{(1 + K_s C_s + K_H C_H)^2}$	$kK_s K_H$
D_I_SH	$\frac{K_{global}C_H C_s}{(1 + K_s C_s + \sqrt{K_H C_H})^3}$	$kK_s K_H$
ND_II_SH	$\frac{K_{global}C_H C_s}{(1 + K_s C_s)(1 + K_H C_H)}$	$kK_s K_H$
D_II_SH	$\frac{K_{global}\sqrt{C_H C_s}}{(1 + K_s C_s)(1 + \sqrt{K_H C_H})}$	$kK_s \sqrt{K_H}$

**Table 3: Langmuir-Hinshelwood kinetic models with four parameters.**

Model	Rate equation ( $-r_s$ )	$K_{global}$
ND_I_SEH	$\frac{K_{global}C_H C_s}{(1 + K_s C_s + K_e C_e + K_H C_H)^2}$	$kK_s K_H$
D_I_SEH	$\frac{K_{global}C_H C_s}{(1 + K_s C_s + K_e C_e + \sqrt{K_H C_H})^3}$	$kK_s K_H$
ND_II_SEH	$\frac{K_{global}C_H C_s}{(1 + K_s C_s + K_e C_e)(1 + K_H C_H)}$	$kK_s K_H$
D_II_SEH	$\frac{K_{global}\sqrt{C_H C_s}}{(1 + K_s C_s + K_e C_e)(1 + \sqrt{K_H C_H})}$	$kK_s \sqrt{K_H}$

The effect of temperature on the specific rate and the adsorption constant was described by the Arrhenius and Van't Hoff equations, respectively, which were used in parameterized forms, given by Equations (3) and (4), to reduce the parametric correlation

(Schwaab and Pinto, 2008). In these expressions,  $T$  is the reaction temperature,  $T_R$  is a reference temperature (80 °C, the mean temperature in the evaluated range),  $R$  is the universal gas constant,  $\delta$  is equal to  $\frac{1}{2}$  for the models with two types of active sites and dissociative hydrogen adsorption and equal to 1 for all other Langmuir-Hinshelwood models, and  $a_i$  and  $b_i$  are the fitting parameters, related to the frequency factor ( $k^0$ ), apparent activation energy ( $E$ ), adsorption constant ( $K_i^0$ ), and heat of adsorption ( $Q_i$ ) as described in Equations (5) – (8).

$$K_{global} = \exp\left(a_{global} + b_{global}\left(1 - \frac{T_R}{T}\right)\right) \quad (3)$$

$$K_i = \exp\left(a_i + b_i\left(1 - \frac{T_R}{T}\right)\right) \quad (4)$$

$$E = RT_R b_{global} - Q_s - \delta Q_H \quad (5)$$

$$Q_i = RT_R b_i \quad (6)$$

$$K_{global}^0 = \exp\left(a_{global} + b_{global}\right) = k^0 K_s^0 \left(K_H^0\right)^\delta \quad (7)$$

$$K_i^0 = \exp\left(a_i + b_i\right) \quad (8)$$

The softwares MATLAB and EMSO (Soares and Secchi, 2003) were employed for parameter estimation and statistical analysis of the obtained experimental data, adopting a confidence interval of 95%. For the evaluation of the effects of pressure and styrene concentration, the parameters were estimated based on 64 data points obtained from 10 experiments at 80 °C (first data set). To evaluate the effect of temperature on styrene hydrogenation, all 116 data points obtained from 18 experiments from both data sets were used. A hybrid optimization method, consisting of the Adaptive Random Search (Secchi and Perlingeiro, 1989) for global search and Flexible Polyhedra (Nelder and Mead, 1965) for solution refinement to a relative accuracy of  $10^{-4}$  for the parameters, was used to solve the maximum likelihood problem, given by the objective function presented in Equation (9), with relative and absolute accuracy of  $10^{-6}$  and  $10^{-8}$ , respectively, for numerical integration of Equations (1) and (2). The hydrogen concentration in the liquid phase was calculated from a simple flash calculation with HYSIS software using the SRK equation of state (Zhou *et al.*, 2006).

$$F_{obj} = \sum_i \sum_j \sum_t \left( \frac{C_{i,j,t}^e - C_{i,j,t}^p}{\sigma_i} \right)^2 \quad (9)$$

where:

$i$  = styrene, ethylbenzene

$j$  = experiment number

$t$  = time (min)

$C_{i,j,t}^e$  = experimental concentration of substance  $i$ , in experiment  $j$  and at time  $t$

$C_{i,j,t}^p$  = predicted concentration of substance  $i$ , in experiment  $j$  and at time  $t$

$\sigma_i$  = standard deviation of  $C_{i,j,t}^e$ .

## RESULTS AND DISCUSSION

### Effect of Pressure and Styrene Concentration

At first, only the effects of hydrogen pressure and styrene concentration were evaluated. In this stage, the estimation of the kinetic parameters was based on the experimental data obtained at 80 °C. Table 4 shows these parameters for the power-law models.

**Table 4: Estimated parameters for the power-law models.**

Model	Specific Rate	$\alpha$	$\beta$	Objective Function	R <sup>2</sup>
PL <sub><math>\alpha\beta</math></sub>	$(8.8 \pm 8.3) \times 10^2$ $L^{1.2}/(\text{mol}^{0.2} \text{ min g}_{\text{cat}})$	0.5±0.1	0.7±0.1	4875.02	0.880
PL <sub><math>\beta</math></sub>	$(1.6 \pm 1.0) \times 10^3$ $L^{1.7}/(\text{mol}^{0.7} \text{ min g}_{\text{cat}})$		0.7±0.1	5933.04	0.855

According to Cheng *et al.* (1986) and Ali (2012), the order of reaction with respect to styrene is 1, corroborating the hypothesis of the PL <sub>$\beta$</sub>  model, whereas Tukac *et al.* (2007) estimated an order of 0.5 for styrene, ratifying the PL <sub>$\alpha\beta$</sub>  model. However, Jackson and Shaw (1995) estimated zero order of reaction with respect to styrene, suggesting that Langmuir-Hinshelwood models are plausible options to represent the reaction rate.

In both power-law models, the order of reaction with respect to hydrogen of 0.7 was close to the value of 0.6 estimated by Vale (2013), and the first order reaction assumed by Cheng *et al.* (1986) and estimated by Tukac *et al.* (2007). Nijhuis *et al.* (2003) also observed a first order with respect to hydrogen

for pressures below 20 bar; with higher hydrogen pressures, the reaction rate stabilized, suggesting the viability of Langmuir-Hinshelwood models. However, our estimated result differs from Ali (2012), which estimated the order of reaction with respect to hydrogen as 0.1, and Jackson and Shaw (1995), which fixed this parameter as zero.

It was observed that the error in the specific rate in both models was very high, in addition to having the lowest coefficients of determination of all evaluated models, suggesting that power-law models do not describe well the experimental data. This occurs because power-law models do not represent accurately the competition for the catalytic sites between the reactants. The fittings of the power-law models to the experimental data are shown in Figure 1.

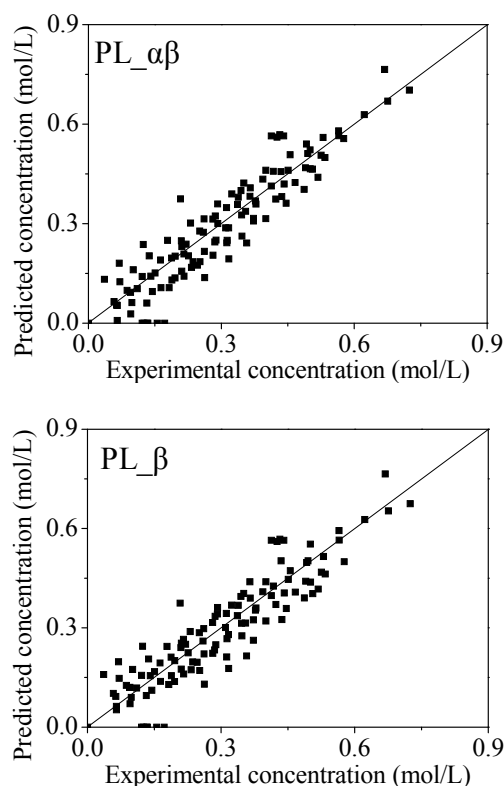


**Figure 1: Fittings of the power-law models.**

Tables 5 to 7 exhibit the estimated parameters for the evaluated Langmuir-Hinshelwood models. The models that considered the adsorption of organic compounds and hydrogen on the same type of catalytic site provided a better fit to the experimental data.

For the models ND\_I\_SE, ND\_II\_SE and D\_II\_SE, it was observed that the errors associated with each parameter are high, showing that these models do not

have statistical significance. In contrast, the model D\_I\_SE presents a good fit to the experimental data and statistically significant parameters, being the best among the models that neglect the hydrogen adsorption.

Regarding the models that consider negligible the ethylbenzene adsorption, whose results are shown in Table 5, it can be seen that the models ND\_I\_SH, D\_I\_SH, and ND\_II\_SH show statistical significance. However, when compared to the other three-parameter models, described in Table 4, it can be seen that these models do not exhibit good fits to the experimental data. In addition, the results for the equilibrium constant for hydrogen adsorption are higher than the values found for the equilibrium constant of styrene adsorption, in disagreement with the literature (Zhou *et al.*, 2007; 2010). In this

respect, only the model D\_II\_SH presents results in accordance with the literature, but the equilibrium constant for hydrogen adsorption is not a significant parameter, given its high confidence interval.

For the four-parameter models, it was found that the models ND\_I\_SEH, D\_I\_SEH and ND\_II\_SEH show statistical significance, while the model D\_II\_SEH presented  $K_H$  equal to zero and with no statistical significance. As demonstrated by the values of the objective function and the determination coefficient, shown in Table 6, the model ND\_I\_SEH best represents the experimental data among the four-parameter models. Its parameters also showed high statistical significance. The fittings of the models ND\_I\_SEH, D\_I\_SEH and ND\_II\_SEH to the experimental data are shown in Figure 2.

**Table 5: Estimated parameters for the Langmuir-Hinshelwood models ND\_I\_SE to D\_II\_SE.**

Model	$K_{global}^1$	$K_s$ (L/mol)	$K_e$ (L/mol)	Objective Function	R <sup>2</sup>
ND_I_SE	38.7 ± 39.3	4.4 ± 3.1	4.3 ± 3.2	3750.71	0.921
D_I_SE	15.6 ± 6.4	1.3 ± 0.4	1.2 ± 0.5	3766.71	0.918
ND_II_SE	37.1 ± 33.4	20.3 ± 19.1	18.6 ± 19.6	3914.63	0.908
D_II_SE	35.4 ± 22.8	73.0 ± 47.8	49.2 ± 39.3	4382.28	0.904

<sup>1</sup>The measurement units of  $K_{global}$  are L<sup>2</sup>/(mol min g<sub>cat</sub>) for the models ND\_I\_SE, D\_I\_SE and ND\_II\_SE and L<sup>1.5</sup>/(mol<sup>0.5</sup> min g<sub>cat</sub>) for the model D\_II\_SE.

**Table 6: Estimated parameters for the Langmuir-Hinshelwood models ND\_I\_SH to D\_II\_SH.**

Model	$K_{global}^1$	$K_s$ (L/mol)	$K_H$ (L/mol)	$k$ (mol/(min g <sub>cat</sub> ))	Objective Function	R <sup>2</sup>
ND_I_SH	10.4±2.2	1.6±0.3	3.2±1.2	2.1	4029.54	0.902
D_I_SH	13.8±3.8	0.9±0.2	1.2±0.9	12.8	4247.60	0.898
ND_II_SH	10.9±3.8	4.2±2.3	5.0±1.2	0.5	4218.79	0.898
D_II_SH	3.2±1.7	6.9±4.8	1.4x10 <sup>-3</sup> ±5.4x10 <sup>-2</sup>	319.4	5676.47	0.873

<sup>1</sup>The measurement units of  $K_{global}$  are L<sup>2</sup>/(mol min g<sub>cat</sub>) for the models ND\_I\_SH, D\_I\_SH and ND\_II\_SH and L<sup>1.5</sup>/(mol<sup>0.5</sup> min g<sub>cat</sub>) for the model D\_II\_SH.

**Table 7: Estimated parameters for the Langmuir-Hinshelwood models with four parameters.**

Model	$K_{global}^1$	$K_s$ (L/mol)	$K_H$ (L/mol)	$K_e$ (L/mol)	$k$ (mol/(min g <sub>cat</sub> ))	Objective Function	R <sup>2</sup>
ND_I_SEH	31.5±14.9	3.6±1.4	4.3±1.9	2.2±0.9	2.0	2985.77	0.934
D_I_SEH	33.3±11.6	1.6±0.5	1.3±0.6	1.2±0.5	15.5	3256.19	0.929
ND_II_SEH	38.7±7.4	16.7±6.0	3.8±1.5	10.7±2.7	0.6	3162.72	0.927
D_II_SEH	35.4±22.8	73.0±47.8	0	49.2±39.3	-	4382.28	0.904

<sup>1</sup>The measurement units of  $K_{global}$  are L<sup>2</sup>/(mol min g<sub>cat</sub>) for the models ND\_I\_SEH, D\_I\_SEH and ND\_II\_SEH and L<sup>1.5</sup>/(mol<sup>0.5</sup> min g<sub>cat</sub>) for the model D\_II\_SEH.

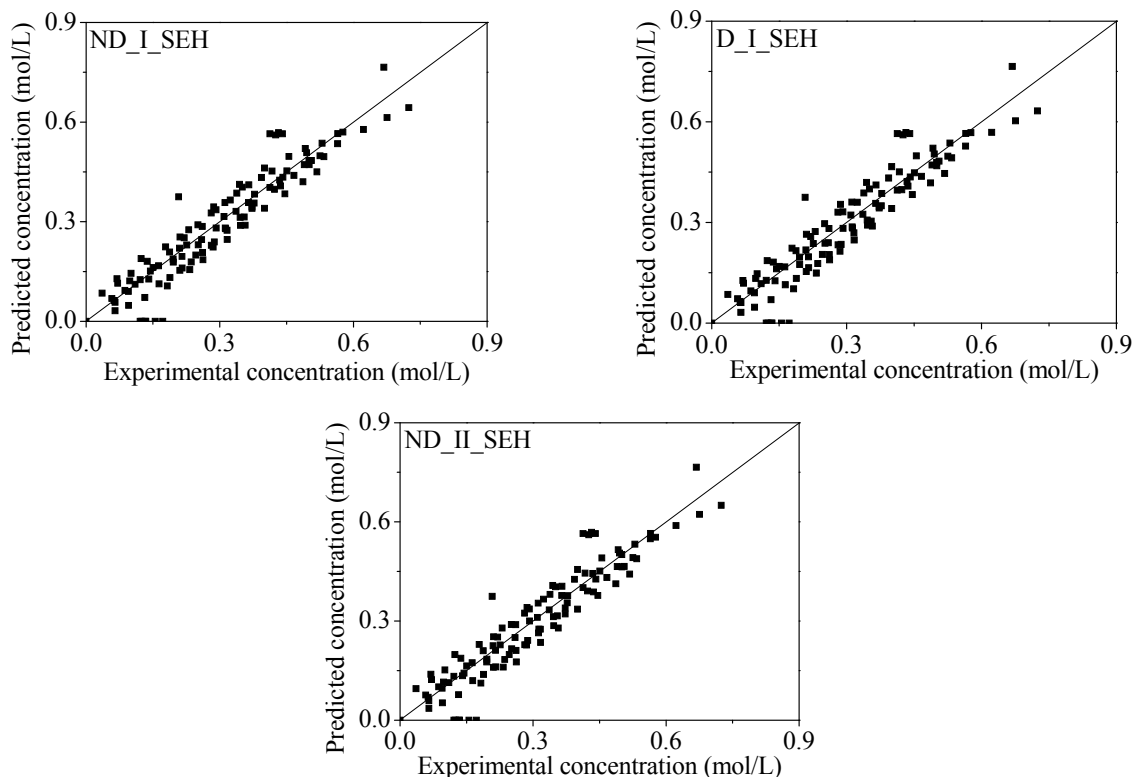


**Figure 2:** Fittings of the Langmuir-Hinshelwood models with 4 parameters.

The equilibrium constants for styrene and hydrogen adsorption estimated in this work can be compared with the ones calculated according to Zhou *et al.* (2007; 2010), conducted in a temperature range of 40–70 °C for the catalyst Pd/Al<sub>2</sub>O<sub>3</sub>. Extrapolating the results to 80 °C, the equilibrium constants for styrene and hydrogen adsorption are equal to 4 L/mol and 32 L/mol, respectively. The first result is similar to that found for the models ND\_I\_SE, ND\_I\_SEH and ND\_II\_SH, but much different from the other models analyzed. According to the results obtained by Nijhuis *et al.* (2003) with a Pd/Al<sub>2</sub>O<sub>3</sub> catalyst at 50 °C, the equilibrium constant for styrene adsorption is  $13.3 \pm 3.1$  L/mol. This result is similar to that for the model ND\_II\_SEH. However, it should be considered that these results were obtained at lower temperatures than this study and the adsorption equilibrium constant behaves inversely proportional to temperature.

Also according to Zhou *et al.* (2007; 2010), the equilibrium constant for hydrogen adsorption assumes values of  $1 \times 10^{-3}$  L/mol to  $4 \times 10^{-3}$  L/mol. These values are in agreement with the model D\_II\_SH, but are much lower than those found in this work for the other models that consider relevant adsorption of hydrogen. However, their results can be compared to the models ND\_I\_SE to D\_II\_SE that neglect the

effects of hydrogen adsorption.

The discrepancies in relation to the works of Zhou *et al.* (2007; 2010) may be due to the different catalyst composition and particle size used in this study (Pd/9%Nb<sub>2</sub>O<sub>5</sub>-Al<sub>2</sub>O<sub>3</sub> powder) and by Zhou *et al.* (2007; 2010), which was egg-shell type Pd/Al<sub>2</sub>O<sub>3</sub>. Furthermore, Zhou *et al.* (2007; 2010) studied the hydrogenation of a mixture of compounds (including styrene), in which there was competition for catalyst sites, a factor that can modify the parameters of the models.

### Effects of Temperature, Pressure and Styrene Concentration

Based on the results with the first experimental data set, it was observed that the models ND\_I\_SE, D\_I\_SE, ND\_I\_SEH, D\_I\_SEH, ND\_II\_SEH and D\_II\_SEH had the best fit to the experimental data and their parameters were in agreement with other works in the field (Nijhuis *et al.*, 2003; Zhou *et al.*, 2007; 2010). Consequently, these models were chosen to investigate the effects of temperature on reaction kinetics. The estimated parameters based on 116 data points from 18 different experiments (both data sets) are presented in Tables 8 and 9.

**Table 8: Estimated parameters for the Langmuir-Hinshelwood models with six parameters.**

Model	ND I SE	D I SE
$a_{global}$	$9.5 \pm 2.1$	$9.0 \pm 2.0$
$b_{global}$	$-14.6 \pm 9.2$	$-52.1 \pm 13.5$
$a_s$	$4.7 \pm 1.1$	$2.9 \pm 0.7$
$b_s$	$-7.2 \pm 4.2$	$-18.4 \pm 6.4$
$a_e$	$4.8 \pm 1.0$	$3.2 \pm 0.7$
$b_e$	$-15.1 \pm 6.7$	$-24.6 \pm 5.8$
Objective Function	7622.09	10196.00
R <sup>2</sup>	0.868	0.826

**Table 9: Estimated parameters for the Langmuir-Hinshelwood models with eight parameters.**

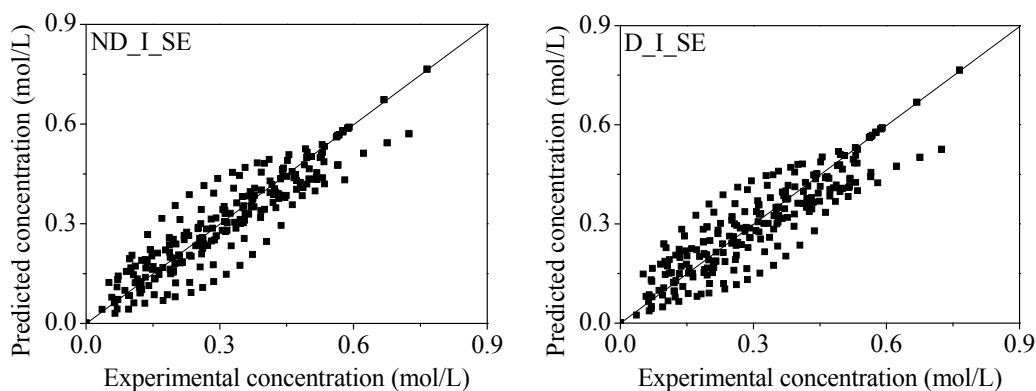
Model	ND I SEH	D I SEH	ND II SEH	D II SEH
$a_{global}$	$2.7 \pm 0.4$	$10.4 \pm 2.4$	$2.7 \pm 0.3$	$4.0 \pm 2.1$
$b_{global}$	$-1.0 \pm 11.2$	$-69.2 \pm 18.8$	$6.4 \pm 6.4$	$-7.6 \pm 136.4$
$a_s$	$0.7 \pm 0.4$	$3.0 \pm 0.8$	$1.7 \pm 0.4$	$4.3 \pm 2.1$
$b_s$	$-3.8 \pm 10.9$	$-22.0 \pm 13.6$	$2.7 \pm 1.8$	$-9.8 \pm 145.7$
$a_H$	$0.4 \pm 1.1$	$6.3 \pm 1.9$	$0.9 \pm 1.0$	$0.0 \pm 3.5$
$b_H$	$-0.1 \pm 31.7$	$-55.1 \pm 14.7$	$3.1 \pm 26.7$	$-0.4 \pm 129.1$
$a_e$	$0.6 \pm 0.3$	$3.3 \pm 0.8$	$1.6 \pm 0.3$	$4.4 \pm 2.1$
$b_e$	$-9.3 \pm 10.1$	$-29.8 \pm 10.9$	$1.4 \pm 13.8$	$-14.9 \pm 140.9$
Objective Function	6559.14	9026.15	6229.48	7418.86
R <sup>2</sup>	0.878	0.843	0.874	0.856

All models with eight parameters presented similar determination coefficients and the model ND\_I\_SEH had the best fit. However, this model, as well as the models ND\_II\_SEH and D\_II\_SEH, has high errors associated with each parameter, showing that these models do not have statistical significance. This can occur because the parameters show high correlation.

It is also possible to notice that the majority of the parameters without statistical significance are of the  $b_i$  kind, which represents the effect of temperature. The large confidence intervals of the parameters suggest that these models are over-parameterized (probably in relation to the equilibrium constant for hydrogen adsorption) and do not reproduce correctly

the effect of temperature.

These problems do not occur for the models ND\_I\_SE and D\_I\_SE in Table 8 and the model D\_II\_SEH in Table 9. The errors associated with each parameter are smaller, which make them more statistically significant. Moreover, the models with six parameters fitted the data well, especially model ND\_I\_SE. This corroborates the works of Zhou *et al.* (2007; 2010), which concluded that the equilibrium constant for hydrogen adsorption is much smaller than the ones of styrene and ethylbenzene. It also supports the hypothesis that the models with eight parameters are over-parameterized. The fittings of the models evaluated to the experimental data are shown in Figure 3.





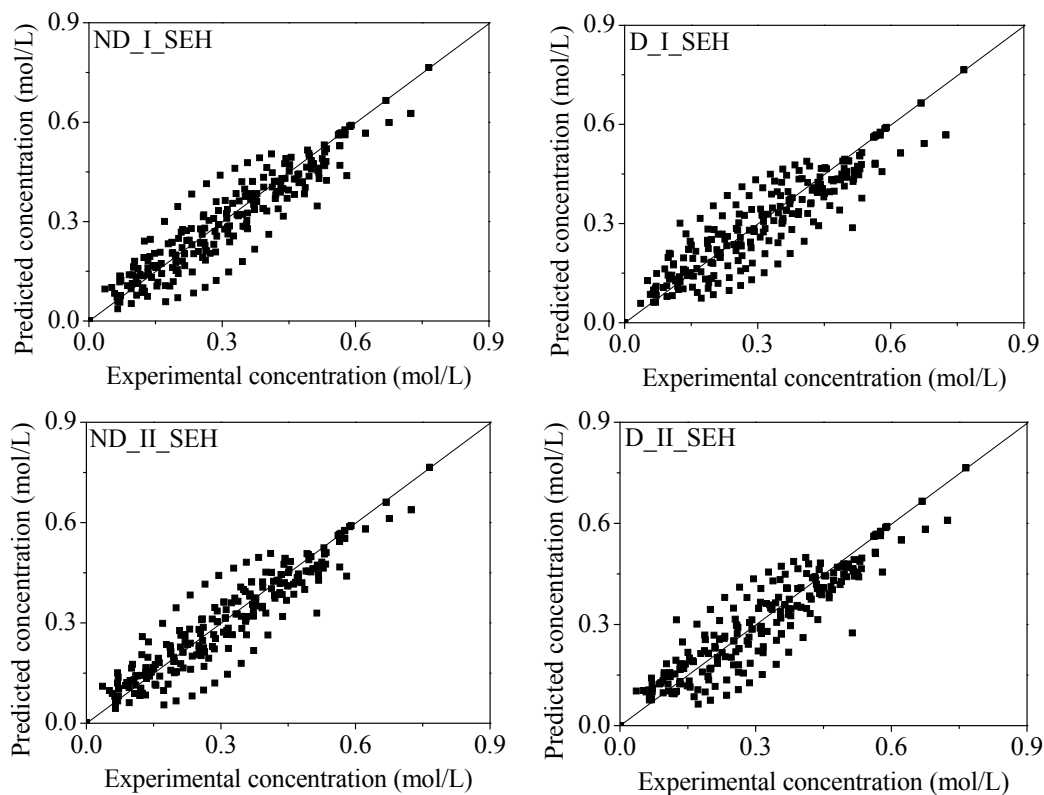


**Figure 3:** Fittings of the Langmuir-Hinshelwood models at several temperatures.

Table 10 shows the values calculated from each model for the apparent activation energy and heat of adsorption. For the models with six parameters, it was impossible to calculate the apparent activation energy and heat of hydrogen adsorption, since the parameters related to the equilibrium constant for hydrogen adsorption were not estimated.

**Table 10: Activation energy and heat of adsorption.**

Model	$Q_s$ (kJ/mol)	$Q_H$ (kJ/mol)	$Q_e$ (kJ/mol)	$E$ (kJ/mol)
ND_I_SE	-21	-	-44	-
D_I_SE	-54	-	-72	-
ND_I_SEH	-11	-0.2	-27	9
D_I_SEH	-65	-162	-87	23
ND_II_SEH	8	9	9	2
D_II_SEH	-29	-1	-44	7

The apparent activation energy calculated for the model D\_I\_SEH presented a value close to those obtained by Nijhuis *et al.* (2003) and Zhou *et al.* (2007; 2010), which are within 26 – 30 kJ/mol. According to Fraga (2009), the apparent activation energy is in the range of 25 – 53 kJ/mol, which is also similar to the model D\_I\_SEH. Corvaisier *et al.* (2013) also

estimated 23 kJ/mol as the apparent activation energy for a Langmuir-Hinshelwood model with the same hypotheses of the model D\_I\_SEH. However, the results of 14.947 kJ/mol obtained by Rojas and Zepieri (2014) and 76.2 kJ/mol estimated by Betti *et al.* (2016) differ from those obtained in this work. For the other models, the values calculated are too small and inconsistent with the apparent activation energy of a chemical reaction (Nijhuis *et al.*, 2003).

The models ND\_I\_SE and D\_II\_SEH provided values for the heat of styrene adsorption close to the value of -24 kJ/mol in the work of Abreu *et al.* (2013). The model ND\_I\_SEH, however, gave results similar to those of Zhou *et al.* (2007; 2010), which were -10.71 kJ/mol and -13.412 kJ/mol, respectively. The models D\_I\_SE and D\_I\_SEH were close to Betti *et al.* (2016), which obtained -54.0 kJ/mol. For the heat of hydrogen adsorption, the result of model D\_I\_SEH was comparable to the studies of Abreu *et al.* (2013) and Betti *et al.* (2016), who found -177 kJ/mol and -108.9 kJ/mol, respectively. Reference values for the heat of ethylbenzene adsorption were found only in the work of Betti *et al.* (2016) as -54.4 kJ/mol, a result relatively close to those of the models ND\_I\_SE and D\_II\_SEH.

Since the model ND\_II\_SEH led to positive values for the heat of adsorption, it is in disagreement with the existing literature (Zhou *et al.*, 2007; 2010). A possible explanation for this anomaly is one of the hypotheses of the model: it considers non-dissociative adsorption of hydrogen. The same consideration is used as a starting point for model ND\_I\_SEH, which gave a heat of hydrogen adsorption very close to zero. This is an indication that this hypothesis is not adequate to predict the phenomenon. Even though good fits were obtained, these models contain parameters without physical significance.

Based on the models evaluated and the corresponding estimated parameters, the equilibrium constants for styrene and hydrogen adsorption were calculated at 80 °C. These values are presented in Table 11 and can be compared with the works of Zhou *et al.* (2007; 2010), using a Pd/Al<sub>2</sub>O<sub>3</sub> catalyst. In these works, the authors obtained 4 L/mol and 32 L/mol, respectively, for the equilibrium constant for styrene adsorption. The first result is similar to the models ND\_I\_SEH and ND\_II\_SEH, but differs greatly from all other models. The second value, though, is close to the models D\_I\_SE and D\_I\_SEH.

**Table 11: Equilibrium constants of styrene and hydrogen adsorption at 80 °C.**

Model	$K_s$ (L/mol)	$K_H$ (L/mol)
ND_I_SE	107.2	-
D_I_SE	18.9	-
ND_I_SEH	2.1	1.5
D_I_SEH	20.4	513.3
ND_II_SEH	5.5	2.5
D_II_SEH	76.1	1

According to Nijhuis *et al.* (2003), also with a Pd/Al<sub>2</sub>O<sub>3</sub> catalyst, at 50 °C, the equilibrium constant for styrene adsorption is  $13.3 \pm 3.1$  L/mol. This result is in agreement with model D\_I\_SE; however, it is necessary to remember that it was obtained at a lower temperature than the ones used in this work, and the equilibrium constant for adsorption decreases as the temperature increases.

In the work of Abreu *et al.* (2013), with a Pd-Ni/Al<sub>2</sub>O<sub>3</sub> catalyst, the equilibrium constant for styrene adsorption at 80 °C is 4.8 L/mol. This value is close to the one obtained by the models ND\_I\_SEH and ND\_II\_SEH.

Fraga (2009) tested a commercial Pd/Al<sub>2</sub>O<sub>3</sub> catalyst at temperatures between 100 – 120 °C, obtaining equilibrium constants for styrene adsorption between 21 – 42 L/mol, which are close to the models D\_I\_SE and D\_I\_SEH.

The values obtained in this work for the equilib-

rium constant for hydrogen adsorption, mainly in the model D\_I\_SEH, are much higher than the values of  $2 \times 10^{-3}$  and  $7 \times 10^{-4}$  L/mol found in the works of Zhou *et al.* (2007; 2010), respectively.

## CONCLUSIONS

This study evaluated kinetic models of the power-law and Langmuir-Hinshelwood types for the hydrogenation of styrene. It was observed that the power-law models cannot describe well the experimental data. Among the evaluated Langmuir-Hinshelwood models, the models ND\_I\_SE and ND\_I\_SEH showed the best fit to the experimental data, which consider the non-dissociative adsorption of hydrogen and adsorption of organic compounds on the same type of catalytic site. However, the last model presented high values for the equilibrium constant for hydrogen adsorption when compared with values found in literature, besides the lack of statistical significance of its parameters.

## ACKNOWLEDGMENTS

We thank CNPq, ANP, FINEP and PRH-13 for the financial support.

## REFERENCES

- Abreu, B. M. N. B., Modesto, F. L. A., Travalloni, L. and Silva, M. A. P., Kinetic modeling of styrene hydrogenation. In Proceedings of EuropaCat-XI, Lyon, France (2013).
- Alegre, V. V., Silva, M. A. P. and Schmal, M., Catalytic combustion of methane over palladium alumina modified by niobia. *Catal. Commun.*, 7, 314 (2006).
- Ali, J., The Hydrogenation of Pyrolysis Gasoline (PyGas) Over Nickel and Palladium Catalysts. Ph.D. Thesis, School of Chemistry University of Glasgow (2012).
- Betti, C., Badano, J., Lederhos, C., Maccarrone, M., Carrara, N., Coloma-Pascual, F., Quiroga, M. and Vera, C., Kinetic study of the selective hydrogenation of styrene over a Pd egg-shell composite catalyst. *Reac. Kinet. Mec. Cat.*, 117, 283 (2016).
- Cheng, Y-M., Chang, J-R. and Wu, J-C., Kinetic study of pyrolysis gasoline hydrogenation over supported palladium catalyst. *App. Catal.*, 24, 273 (1986).
- Corvaisier, F., Schuurman, Y., Fecant, A., Thomazeau, C., Raybaud, P., Toulhoat, H. and Farrusseng, D.,

- Periodic trends in the selective hydrogenation of styrene over silica supported metal catalysts. *J. Catal.*, 307, 352 (2013).
- Fraga, E. B., Modelagem de um Reator de Hidrogenação de Gasolina de Pirólise Industrial. M. Sc. Thesis, COPPE, Universidade Federal do Rio de Janeiro (2009). (In Portuguese).
- Gaspar, A. B., Santos, G. R., Costa, R. S., Silva, M. A. P. and Britto, J. M., Hydrogenation of synthetic PYGAS—Effects of zirconia on Pd/Al<sub>2</sub>O<sub>3</sub>. *Catal. Today*, 133, 140 (2008).
- Hoffer, B. W., Bonné, R. L. C., Langeveld, A. D., Griffiths, C., Lok, C. M. and Moulijn, J. A., Enhancing the start-up of pyrolysis gasoline hydrogenation reactors by applying tailored ex situ presulfided Ni/Al<sub>2</sub>O<sub>3</sub> catalysts. *Fuel*, 83, 1 (2004).
- Jackson, S. D. and Shaw, L. A., The liquid-phase hydrogenation of phenyl acetylene and styrene on a palladium/carbon catalyst. *App. Catal. A: Gen.*, 134, 91 (1996).
- Medeiros, J. L., Araújo, O. Q. F., Gaspar, A. B., Silva, M. A. P. and Britto, J. M., A kinetic model for the first stage of PYGAS upgrading. *Braz. J. of Chem. Eng.*, 24, 119 (2007).
- Mostoufi, N., Ahmadpour, M. and Sotudeh-Gharebagh, R., Modelling the two-stage pyrolysis gasoline hydrogenation. *Comp. Aid. Chem. Eng.*, 20, 451 (2005).
- Nelder, J. A. and Mead, R., A Simplex method for function minimization. *The Comp. J.*, 7(4), 308 (1965).
- Nijhuis, T. A., Dautzenberg, F. M. and Moulijn, J. A., Modeling of monolithic and trickle-bed reactors for the hydrogenation of styrene. *Chem. Eng. Sci.*, 58, 1113 (2003).
- Rojas, M. and Zeppieri, S., Simulation of an industrial fixed-bed reactor with cocurrent downflow for hydrogenation of PYGAS. *Catal. Today*, 220, 237 (2014).
- Schwaab, M. and Pinto, J. C., Optimum reparameterization of power function models. *Chem. Eng. Sci.*, 63, 4631 (2008).
- Secchi, A. R. and Perlingeiro, C. A. G., Otimização: Busca Aleatória Adaptativa. *Anais do XII Congresso Nacional de Matemática Aplicada e Computacional (XII CNMAC)*, São José do Rio Preto, SP, 49 (1989). (In Portuguese).
- Soares, R. P. and Secchi, A. R., EMSO: A New Environment for Modelling, Simulation and Optimization. *ESCAPE* 13, 947 (2003).
- Tukac, V., Simícková, M., Chyba, V., Lederer, J., Kolena, J., Hanika, J., Jiricny, V., Stanek, V. and Stavárek, P., The behavior of pilot trickle-bed reactor under periodic operation. *Chem. Eng. Sci.*, 62(18-20), 4891 (2007).
- Vale, C. S. A., Hidrogenação de gasolina de pirólise empregando catalisadores à base de paládio. Final Project, Escola de Química, Universidade Federal do Rio de Janeiro (2013). (In Portuguese).
- Wen, X., Li, R., Yang, Y., Chen, J. and Zhang, F., An egg-shell type Ni/Al<sub>2</sub>O<sub>3</sub> catalyst derived from layered double hydroxides precursor for selective hydrogenation of pyrolysis gasoline. *App. Catal. A: Gen.*, 468, 204 (2013).
- Wolffenbuttel, B. M. A., Nijhuis, T. A., Stankiewicz, A. and Moulijn, J. A., Influence of water on fast hydrogenation reactions with monolithic and slurry catalysts. *Catal. Today*, 69, 265 (2001).
- Zeng, T. Y., Zhou, Z. M., Zhu, J., Cheng, Z. M., Yuan, P. Q. and Yuan, W. K., Palladium supported on hierarchically macro-mesoporous titania for styrene hydrogenation. *Catal. Today*, 147S, S41 (2009).
- Zhou, Z., Cheng, Z., Cao, Y., Zhang, J., Yang, D. and Yuan, W., Kinetics of the selective hydrogenation of pyrolysis gasoline. *Chem. Eng. Technol.*, 30, 105 (2007).
- Zhou, Z., Cheng, Z., Yang, D., Zhou, X. and Yuan, W., Solubility of hydrogen in pyrolysis gasoline. *J. Chem. Eng.*, 51, 972 (2006).
- Zhou, Z., Zeng, T., Cheng, Z. and Yuan, W., Kinetics of selective hydrogenation of pyrolysis gasoline over an egg-shell catalyst. *Chem. Eng. Sci.*, 65, 1832 (2010).